

**Military Technical College**  
**Kobry El-Kobbah,**  
**Cairo, Egypt**



**8<sup>th</sup> International Conference**  
**on Electrical Engineering**  
**ICEENG 2012**

## A Novel TSA Array for Automotive Radars at 79 GHz

Ahmed Nafe, 5<sup>th</sup>year -Student GUC, Dipl. Eng. Micheal Frei, Ulm University, Member *IEEE*.

### **Abstract:**

The shift of the frequency band assigned for automotive radars from 24 GHz to 79 GHz led to an increased research in the area of design of radars that operate at the new band from 76 to 81 GHz. The antenna plays a key role in the operation of a radar sensor. Designing an antenna that provides high directivity and low side lobe level and at the same time to be small in size and of low manufacturing cost in mass production is a challenging task for researchers. In this work, investigations on Tapered Slot Antenna (TSA) arrays operating at 79 GHz suitable to meet automotive radars demands were carried out. A Fermi-Dirac based TSA was studied parametrically and optimized with the aid of CST microwave studio. The optimized design was fabricated along with its attached feeding structures and shielded housing to suppress unwanted feed radiation. The measurement of reflection coefficient indicated wideband behavior ( $< -10\text{dB}$ ) extending nearly over the whole E-band. Despite its small size (3.75 by 7.5 mm) the antenna showed fairly high gain (10 dB). A 4 -element E-plane array was built and a parallel feeding network was optimized to feed the array elements with equal amplitudes and phases. The array was fabricated and measured showing a gain of 13.8 dB and a side lobe level of 14 dB indicating that it is attractive candidate for employment in automotive radar sensors, especially when the number of the array elements is increased.

## **Introduction:**

In 2005, the commission of European community allocated the frequency range from 21.65 to 26.65 GHz for Ultra-Wide Band (UWB) Short Range Radar (SRR). Due to the overlap of this band with existing systems such as the unlicensed ISM (Industrial, Scientific and Medical) band, the frequency regulation for UWB SRR was redefined [4]. The marketing of the 24GHz radar systems shall be stopped by June 2013. Automotive radars shall then operate at a new allocated frequency of 79 GHz with a bandwidth range from 77 to 81GHz [1-4].

Tapered slot antennas (TSAs) are planar antennas which can be fabricated through standard printed circuit board process. This effectively reduces production cost and makes them suitable for mass production. Also, they can be easily integrated with other active planar circuits. They are known to provide intermediate to high directionality and easy integration in antenna arrays. All these features make them attractive candidates for implementation in radar sensors.

(TSAs) are derived from an ordinary slot line by continuously widening the slot along the line length in a smooth manner. The slot line is operated in its fundamental mode, namely the slot mode. As TSAs are operated in traveling wave modes, they produce end-fire radiation pattern with linear polarization parallel to the plane of the substrate. The E-plane of the antenna is parallel to the substrate while the H-plane is orthogonal to it [5,6].

In this work the Fermi function based taper profile is studied. Taper details and comparison of simulated and measured results are provided in sections (I) and (II). Fabrication of designed antennas has been carried out in the lab of the Institute of Microwave Techniques at the University of Ulm, Germany. In section (III), the measured and simulated results of 4-element E-plane array constructed out of the Fermi antenna are discussed. The chosen

substrate is ROGERS 3003 with  $\epsilon_r = 3$  and thickness of 127  $\mu\text{m}$ . Finally, conclusion and future work is presented in section (IV).

**(I) The Fermi Taper:**

The Fermi taper is based on the Fermi-Dirac distribution function. Its basic form is given by:

$$y = \frac{A}{1 + e^{-bx}} \tag{1}$$

Where,

$$A = \frac{W_{\min}}{2} [1 + e^{bL/2}] \tag{2}$$

$$b = \frac{2}{L} \ln \left( \frac{W_{\max}}{W_{\min}} \right) \tag{3}$$

This design was reported by Sugawara et. al. [7] to have more symmetrical beams and lower side lobes than exponentially tapered slot antennas. It can be viewed as an improvement over the Vivaldi antenna introduced by Gibson in [8]. As seen in equations 1, 2, the Fermi function employs an exponential term within its definition. The dimension of the optimized design is given table (1) and is schematically presented in figure (1). Both outer edges of the metallization were corrugated to allow further reduction in size and suppress the backward creeping wave [9-12]. The corrugation parameters are  $\bar{p}$ ,  $d$  and  $\delta$  (slot width to pitch ratio), as shown in Figure (1).

Parameter	Value
$W_{max}$	2.5 mm
$W_{tot}$	3.75 mm
$L$	7.5 mm
$W_{min}$	100 $\mu\text{m}$
$\bar{p}$	0.75
$d$	0.7 mm
$\delta$	0.7

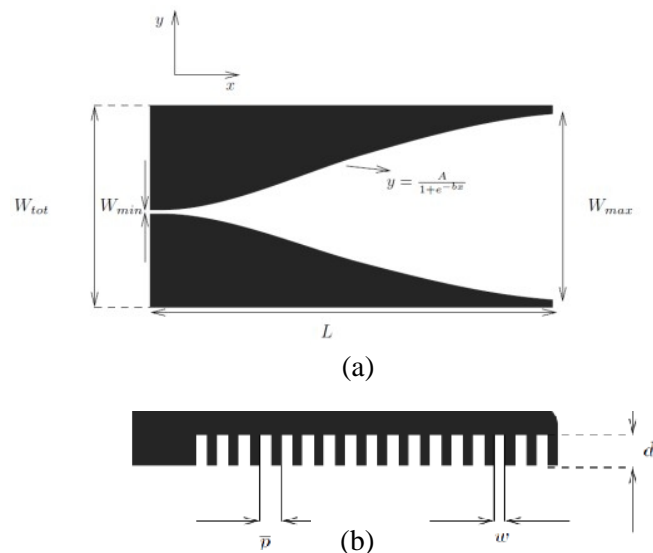


Table (1) Optimized dimensions of Fermi Design

Figure (1) A schematic Fermi structure (a) and side corrugation (b)

The feeding structure, as seen in figures 3,4, is done via a WR12 waveguide by using a transition from the waveguide to differential microstrip line (DMSL) followed by another transition from DMSL to slotline.

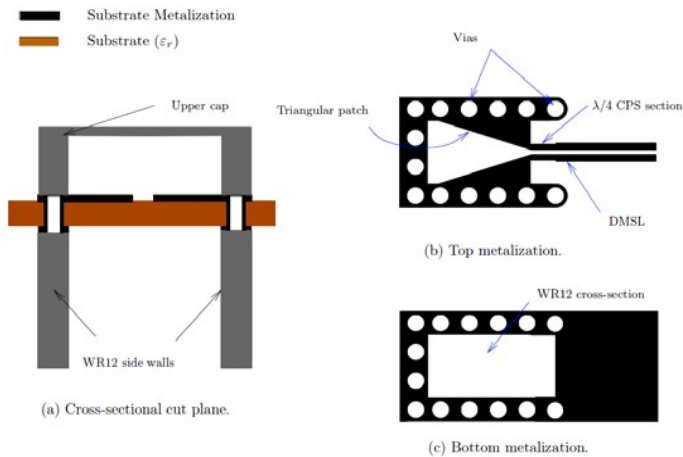


Figure (3) 2-D views of the RWG to DMSL transition.

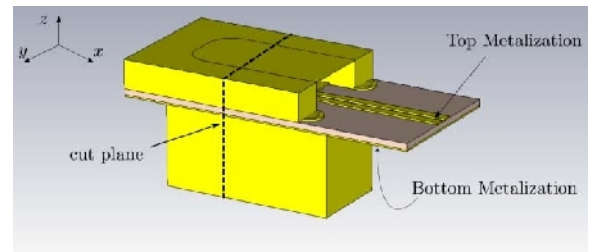


Figure (4) 3-D view of the RWG to DMSL transition.

Details about the transition design can be found in [13]. A shielded housing is used to accommodate both to minimize any feed radiation. A photo for the fabricated Fermi antenna is shown Figure (5).

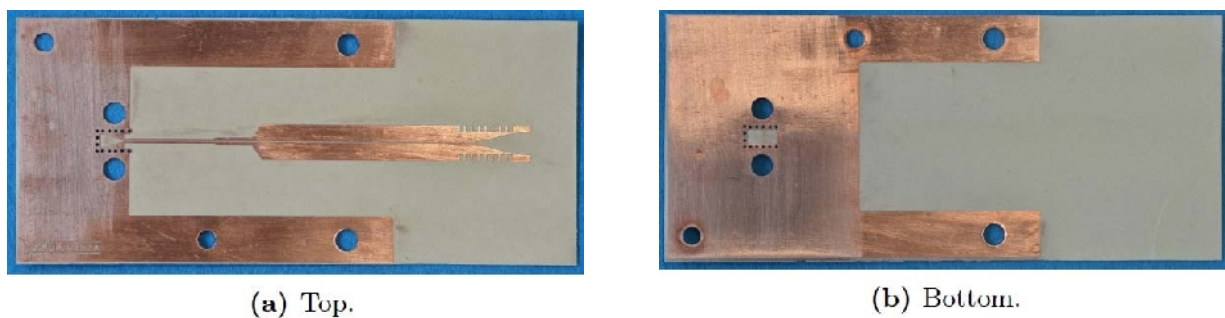


Figure (5) Fabricated Fermi antenna

As shown in Figure (6), the measured return loss is better than 20 dB at 79 GHz and is in well agreement with the simulated values over the desired band 76 to 81 GHz.

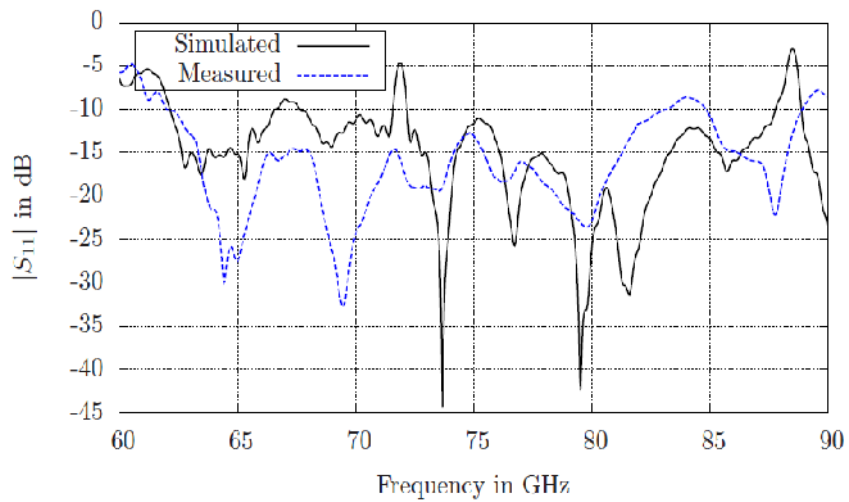


Figure (6) Simulated and measured return loss for the Fermi antenna.

The E and H plane radiation patterns were measured at 79 GHz and are graphically represented together with the predicted simulated patterns in figure (7). The measured gain is 9.5 dB while the simulated one is 11 dB. The decrease in measured gain is due to increase of the value of substrate tangent loss at 79 GHz than the value given by the supplier at 10 GHz which was used when modeling for the simulation.

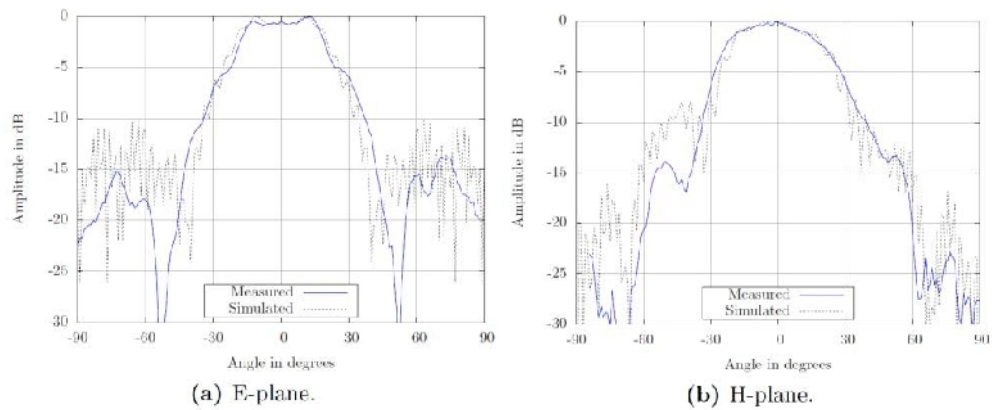


Figure (7) Simulated and measured radiation pattern of the Fermi antenna at f= 79 GHz

**(II) TSA array :**

Using the corrugated Fermi antenna, a 4 element linear array in the E-plane fed by a corporate feeding network is designed, fabricated and measured. The array elements are excited with equal amplitudes and phases.

The power division is done through a microstrip network. Then a microstrip to slotline balun is used to transfer the power to the corresponding elements. The Simulated insertion loss at 79 GHz was -7.25 dB indicating a -1.25 dB loss in the power division stage and the excitation phase of the elements were within 5° from each other, as shown in Figure(8).

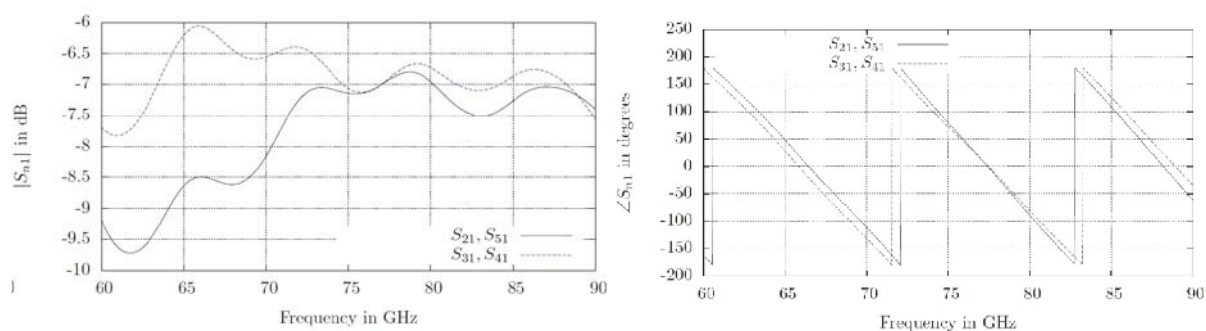


Figure (8) Simulated S-parameters of the desired feeding network

The fabricated array is shown in Figure (9).

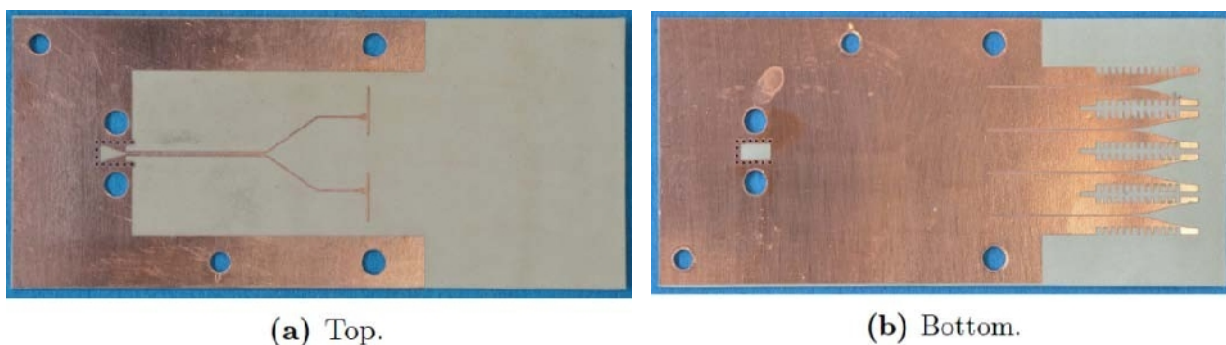


Figure (9) The fabricated Fermi antenna array

**(III) Array Results:**

The simulated and measured return loss of the array is shown in Figure (10). The measured return loss is observed to have the same profile as the simulated one but is shifted in frequency by approximately 1GHz towards higher frequencies. This shift might be due to inaccurate modeling of the dielectric dispersion of the substrate in the simulation. The antenna is matched satisfactorily at 79GHz with nearly 11 dB return loss.

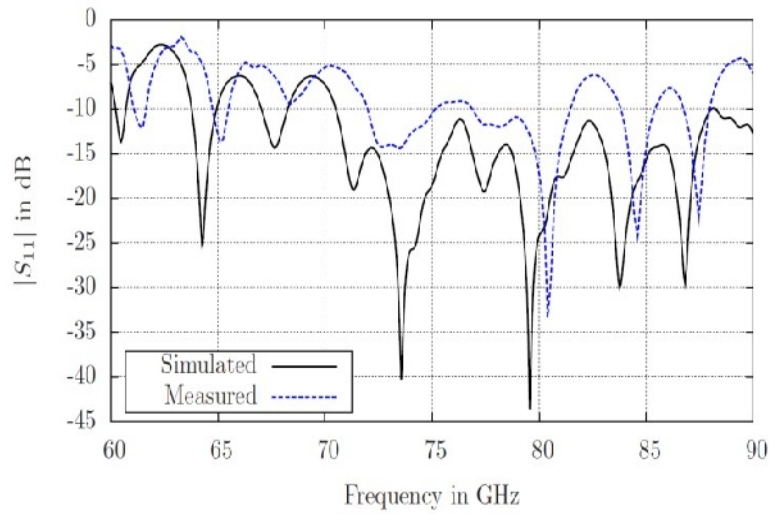


Figure (10) Simulated and measured return loss for the Fermi antenna array.

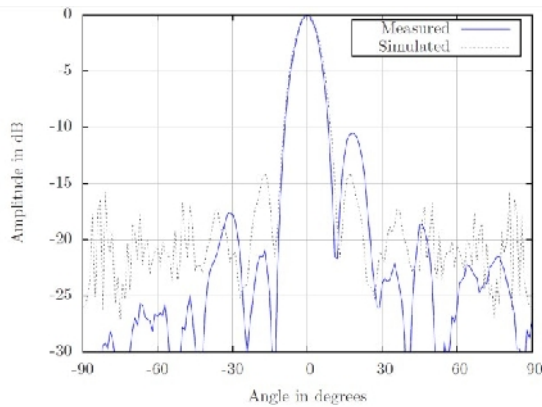


Figure (11) Simulated and measured E-plane pattern for the Fermi array antenna at 79 GHz.

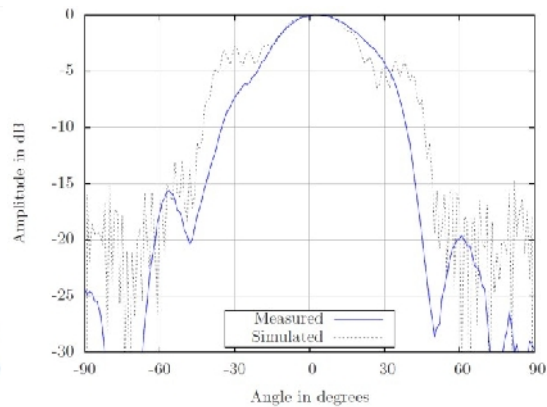


Figure (12) Simulated and measured H-plane pattern for the Fermi array antenna at 79 GHz.

The simulated and measured E-plane normalized patterns are shown in Figure (11). The main beam is nearly the same for both. An asymmetry is observed in the measured pattern where the left side lobe is diminished by approximately 6 dB. Also the right side lobe has a higher magnitude than predicted in the simulation. This asymmetry might be caused by an unbalance in power distribution between the elements or by an asymmetry in the configuration.

Simulated and measured E-plane pattern for the Fermi antenna array at 79GHz. The H-plane is depicted in Figure (12). The measured pattern shows a strong deviation in the main beam compared to the simulations. This might be due to the approximate model of the shielding used in the simulation. Nevertheless, the positions of nulls are predicted accurately by the simulations.

The measured gain is approximately 13.8 dB this is about 2.5 dB below the expected gain from the simulation. This might be due to the increased substrate loss at 79GHz. Also, a possible source of loss that is not accounted for is the surface roughness of the microstrip. This loss mechanism is more effective at 79GHz than at low frequencies.

#### **(IV) Conclusion:**

To examine the capabilities of TSAs as array elements in automotive radar antennas, the Fermi antenna was integrated in a 4 element E-plane array. A parallel feeding network was designed to feed the array elements with equal amplitudes and phases. The array was fabricated and measured and satisfactory agreement with simulated results was obtained. The array design presented showed good performance in terms of gain, side lobe level and matching indicating that it is attractive candidate for employment in automotive radar sensors, especially when the number of the array elements is increased. The use of the shielding caused appreciable distortion in the radiated beams even when covered with absorbing material. The proposed designs had a comparable E-and H-plane beamwidth.

As a step forward, TSAs could be combined with a lens in order to focus and narrow the H-plane beam and increase the gain of the antenna. Also, antipodal versions of the designs presented in this work could be investigated. Especially the possibility of integrating them with a substrate integrated waveguide feed. This would eliminate any radiation from the feed and consequently the need of any shielding.

#### **References:**

- [1] R. Abou-Jaoude and M. Grace. Test systems for automotive radar. In Vehicular Technology Conference Proceedings, 2000. VTC 2000-Spring Tokyo. 2000 IEEE 51st, volume 1, pages 492 –495 vol.1, 2000.
- [2] M. Köandhler, F. Gumbmann, J. Schüandrer, L.-P. Schmidt, and H.-L. Blöandcher. Considerations for future automotive radar in the frequency range above 100 ghz. In German Microwave Conference, 2010, pages 284 –287, march 2010.
- [3] V. Jain, F. Tzeng, Lei Zhou, and P. Heydari. A single-chip dual-band 22-to-29ghz/77-to-81 ghz bicomos transceiver for automotive radars. In Solid-State Circuits Conference –

- Digest of Technical Papers, 2009. ISSCC 2009. IEEE International, pages 308 –309,309a, feb. 2009.
- [4] E.G. Hoare and R. Hill. System requirements for automotive radar antennas. In *Antennas for Automotives* (Ref. No. 2000/002), IEE Colloquium on, pages 1/1 –111, 2000.
- [5] S.B. Cohn. Slot line on a dielectric substrate. *Microwave Theory and Techniques, IEEE Transactions on*, 17(10):768 – 778, oct 1969.
- [6] D. Schaubert, E. Kollberg, T. Korzeniowski, T. Thungren, J. Johansson, and K. Yngvesson. Endfire tapered slot antennas on dielectric substrates. *Antennas and Propagation, IEEE Transactions on*, 33(12):1392 – 1400, dec 1985.
- [7] S. Sugawara, Y. Maita, K. Adachi, K. Mori, and K. Mizuno. A mm-wave tapered slot antenna with improved radiation pattern. In *Microwave Symposium Digest, 1997.*, IEEE MTT-S International, volume 2, pages 959 –962 vol.2, jun 1997.
- [8] P. J. Gibson. The Vivaldi aerial. 9th Eur. Microw. Conf. , Vol. 31:101 – 105, 1979.
- [9] Valeri Mikhnev and Pertti Vainikainen. Wideband tapered-slot antenna with corrugated edges for gpr applications. In *Microwave Conference, 2003. 33rd European*, pages 727 – 729,oct. 2003.
- [10] M.E. Bialkowski and Yifan Wang. A size-reduced exponentially tapered slot antenna with corrugations for directivity improvement. In *Microwave Conference, 2009. APMC 2009. Asia Pacific*, pages 2482 –2485, dec. 2009.
- [11] C. Granet and G.L. James. Design of corrugated horns: a primer. *Antennas and Propagation Magazine, IEEE*, 47(2):76 – 84, april 2005.
- [12] S. Sugawara, Y. Maita, K. Adachi, K. Mori, and K. Mizuno. Characteristics of a mm-wave tapered slot antenna with corrugated edges. In *Microwave Symposium Digest, 1998 IEEE MTT-S International*, volume 2, pages 533 –536 vol.2, jun 1998.
- [13] Z. Tong, A. Stelzer, W. Menzel, C. Wagner, R. Feger, and E. Kolmhofer. A wide band transition from waveguide to differential microstrip lines. In *Microwave Conference, 2008. APMC 2008. Asia-Pacific*, pages 1 –4, dec. 2008.
- [14] B. Shuppert. Microstrip/slotline transitions: modeling and experimental investigation. *Microwave Theory and Techniques, IEEE Transactions on*, 36(8):1272 –1282, aug 1988.